Biosilicate and marine spongin in the process of healing of tibial bone defects in rats

Biosilicato e espongina marinha no processo de cicatrização de defeitos ósseos tibiais em ratos

Hueliton Wilian Kido[1], Kelly Rossetti Fernandes[2], Bianca Priscilla Dorileo Fermino[2], Cintia Pereira de Goes Santos[2], Giovanna Caroline Aparecida do Vale[2*], Matheus de Almeida Cruz[2], Ingrid Regina Avanzi[2], Julia Risso Parisi[3], Angela Maria Paiva Magri[2], Carlos Alberto Fortulan[3], Edgar Dutra Zanotto[3], Oscar Peitl[3], Renata Neves Granito[2], Ana Claudia Muniz Rennó[2]

[1] University Nove de Julho (UNINOVE), Mauá, SP, Brazil
[2] Federal University of São Paulo (UNIFESP), Santos, SP, Brazil
[3] Federal University of São Carlos (UFSCar), São Carlos, SP, Brazil
*Corresponding author: gica.vale@hotmail.com

ABSTRACT

The objective of the current study is to evaluate the orthotopic in vivo response to Biosilicate/Spongin composites. Wistar rats (24) were submitted to a tibial bone defect and distributed in the Control-CG, Biosilicate-BS and Biosilicate/Spongin-BS/SPG groups. The histological analysis demonstrated that BS stimulated newly formed bone ingrowth into the defect area and animals treated with BS/SPG showed an intense amount of granulation. BS/SPG showed lower values of %BV/TV (8.8 and 3.1 times less than CG and BS, respectively) and N.Ob/T.Ar. (3.8 and 4 times less than CG and BS, respectively). The immunohistochemistry analysis demonstrated no difference between Runx-2 and Rank-L immunostaining. Additionally, the biomechanical test demonstrated similar values for all the groups. This current study concluded that the BS is a promising material to be used as bone graft substitute. However, BS/SPG, in the proportion used, did not have a positive influence in the amount of newly formed bone in tibial bone defects.

Keywords: Biomaterials; Biomedical application; Marine Biotechnology; Spongin; Tissue Engineering;

RESUMO

O estudo avaliou a resposta ortotópica *in vivo* de compósitos de Biosilicato/Espongina. Ratos wistar (24) foram submetidos a um defeito ósseo tibial e distribuídos nos grupos Controle-CG, Biosilicato-BS e Biosilicato/Espongina-BS/SPG. A análise histológica demonstrou que o BS estimulou o crescimento ósseo neoformado na área do defeito e os animais tratados com BS/SPG mostraram uma quantidade intensa de tecido de granulação. BS/SPG apresentou valores menores de %BV/TV (8,8 e 3,1 vezes menor do que CG e BS, respectivamente) e N.Ob/T.Ar (3,8 e 4 vezes menor do que CG e BS, respectivamente). A análise de imunoistoquímica não demonstrou diferença entre os grupos para Runx-2 e Rank-L. O teste biomecânico demonstrou valores semelhantes para todos os grupos. O estudo concluiu que o BS é um material promissor para ser utilizado como substituto do enxerto ósseo. Porém, o BS/SPG, na proporção utilizada, não influenciou positivamente na quantidade de osso neoformado em defeitos tibiais.

Palavras-chave: Aplicação biomédica; Biomateriais; Biotecnologia Marinha; Engenharia de Tecidos; Espongina

INTRODUCTION

Worldwide, accidents, traumas, sport injuries and diseases are responsible by enormous orthopedic burdens, most of each is related to bone fractures (EZIRGANLI et al., 2015). In general, bone tissue has the intrinsic ability of self-repairing but there are many circumstances where full bone regeneration fails, requiring an additional treatment mainly surgeries for bone graft implantation (AMINI et al, 2012; HENCH and JONES, 2015).

Bone substitutes are manufactured from biomaterials, which have the ability of stimulating bone tissue ingrowth and metabolism, accelerating fracture consolidation (BOSSINI et al., 2011; FERNANDES et al., 2017). One of the most promising class of biomaterials is bioceramics which includes a broad range of inorganic/nonmetallic compositions, such as hydroxyapatite, bioactive glass, calcium phosphate, and others (HENCH and JONES, 2015; KIDO et al., 2014).

Bioactive glasses, including Biosilicate® (BS), have been employed, in experimental studies and in the clinical setting, as promising bone substitute materials, able of accelerating the process of bone healing (MATSUMOTO et al., 2012). BS, in the composition of P2O5-Na2O-CaO-SiO2 system, has the ability to integrate with bone tissue, forming an active layer of hydroxycarbonate apatite (HCA), with similar characteristics those of apatite found in bone (MOURA et al., 2007; KIDO et al., 2015). Due to these properties, many authors have showed that BS presents stimulatory effects on bone cell proliferation and on the acceleration of fracture healing (COLE et al., 2011; LIAO et al., 2004; OLIVEIRA et al., 2009; PINTO et al., 2013; REZWAN et al., 2006; RIZWAN et al., 2017; SILVA et al., 2014; ZHAO et al., 2015).

In spite of all the stimulatory effects of BS on bone tissue metabolism, in more severe injuries such a bone defect of large dimensions or osteoporosis-related fractures, the osteoinductive properties of the glass may not be sufficient to stimulate bone tissue healing (LIN et al., 2011). Due to this reason, BS composite scaffolds have been developed with the addition of an organic part in order to optimize the biological properties of the grafts (EINHORN, 2011; KIDO et al., 2019; PETTIAN et al., 2018). One of the most promising strategy in this field is combining BS (the mineral component) with collagen (representing the organic part) (DROSSE et al., 2008).

Collagen is the most common protein in the vertebrates and it has been widely used for tissue engineering applications (GREEN et al., 2003; WILLIAMS, 2006). Many different sources of collagen have been explored mainly the one extracted from bovine and porcine bone and skin (HÄGG et al., 2001; IWATSUBO et al., 2015). However, some issues are related to their use, especially the high costs linked to the material production and the risk of some disease transmission (EXPOSITO et al., 2002; PARISI et al., 2019; SWATSCHEK et al., 2002).

As an alternative, innovative new raw materials have been explored such as the use of marine collagen including the ones from fishes, shrimps and jellyfishes (LOPEZ-HEREDIA et al., 2012; WANG et al., 2013). Furthermore, collagen from marine sponges (also called spongin- SPG) has also been demonstrated to be biocompatible and able of supporting human skin cell growth (CAPUZZO et al., 2015; LOPEZ-HEREDIA et al., 2012; WANG et al., 2013). Some authors have demonstrated that SPG seems to be able of accelerating osteoblast cell proliferation in in vitro studies, showing an osteogenic potential (LOPEZ-HEREDIA et al., 2012; SHIN et al., 2003; WANG et al., 2013). Similarly, bone graft composites manufactured with SPG have also been studied. Parisi et al. (2018) demonstrated that combining SPG with hydroxyapatite (HA) (HA/SPG in the proportion of 70% and 30%, respectively) was able of increasing osteoblast and fibroblast cell viability compared to HA only, highlighting the potential of the introduction of SPG into HA to improve the performance of the graft for bone regeneration applications.

In view of the growing need and interest in manufacturing composites with improved osteogenic properties to be used as off-the-shelf bone substitutes, it was hypothesized that the addition of SPG into BS samples might constitute an innovative way of improving material performance. Despite these possible advantages, there is still limited understanding of the interactions between BS and SPG. Thus, the aim of the current study is to evaluate the orthotopic in vivo response to BS/SPG using a tibial defect in rats. Histological and histomorphometric analysis, immuhistochemistry and biomechanical tests were performed to evaluate the effects of implants on defects 15 days post-surgery.

MATERIAL AND METHODS

Materials

BS (size 250-1000 μm) was provided by Vitreous Materials Engineering, Federal University of Sao Carlos, São Carlos, São Paulo, Brazil.

SPG was extracted from the *Aplysina fulva* marine sponge. Specimens were collected in locations (Praia Grande, 23º49'23.76 "S, 45º25'01.79 "W and in Araçá Bay area, 23º81'73.78 "S, 45º40'66.39 "W, both in São

Sebastião, São Paulo, Brazil). SPG extraction was based on a method previously described and successfully used (HUANG et al., 2011; MAGRI et al., 2015; KUTTAPPAN et al., 2016). Briefly, samples, after collection were immediately washed with sea water and transported to the laboratory. After that, 3 washing steps were performed in Milli-Q water for removing cell debris and were cut into pieces, being placed in Tris-HCl buffer (100 mM, pH 9.5, 10 mM EDTA, 8 M urea, 100 mM 2-mercaptoethanol). With the addition of NaOH, the pH was adjusted to 9 and the solution was transferred to a stirred beaker (for 24hrs). After that, solution was centrifuged (5000 g; 5 minutes and 2ºC) and the pellet was discarded, being the supernatant removed. Acetic acid solution was added until the pH reaching 4. A precipitate was formed and resuspended in Milli-Q water, centrifuged again and lyophilized for preservation (MAGRI et al., 2015).

Also, the following materials were used for scaffold manufacturing: carboxymethyl cellulose (CMC, density 1.59 g/cm3, Sigma Aldrich, Missouri, USA), Polymethyl methacrylate (PMMA, particle size: 15 µm) and methyl methacrylate (MMA, purity: 99.09%) (both from VIPI Produtos Odontológicos, Pirassununga, São Paulo, Brazil).

Scaffold manufacturing

Porous scaffolds of BS and BS/SPG (in the proportion of 70% and 30%, respectively) were used in this study (porosity around 60%). Briefly, materials (BS, SPG, PMMA and CMC), in powder, were weighed and mixed in a silicone container using a spatula, at the different proportions (Table 1). PMMA was used to aggregate the materials and CMC used as a porogenic material (37, 38). Distilled water was added and powders were mixed, followed by the addition of MMA monomer (used as a crosslink agent). Mixture was rapidly transferred to a silicon mold (3 mm diameter x 2 mm height), sealed and submitted to a pressure air chamber (at 0.6 MPa) (30 mins) and vacuum dried (10-3 Torr) for 15 mins. At the end, composites were removed from the silicon molds, packaged and sterilized by ethylene oxide (Acecil, Campinas, SP, Brazil).

Table 1. Scaffold formulation expressed in grams (g). Polymethyl methacrylate (PMMA), Methyl methacrylate (MMA), Biosilicate (BS), Spongin (SPG), Carboxymethyl cellulose (CMC).

Groups	PMMA(g)	MMA(g)	BS(g)	SPG(g)	CMC(g)	Water(g)
BS	0.236	0.472	0.560	0.000	0.043	0.565
BS/SPG 70/30	0.236	0.472	0.455	0.051	0.043	0.565

SEM morphology

For morphological analysis of the scaffolds, the scanning electron microscope (SEM) (LeO 440, Carl Zeiss, Jena, Germany) was used (10 KeV electron beam). Samples were mounted on aluminum stubs with carbon tape and sputter-coated with gold prior to examination.

In vivo experiments

All the protocols and procedures used were approved by Animal Care Committee guidelines of the Federal University of São Paulo (2017/9664130417). Twenty-four healthy male Wistar rats (12 weeks, weight 300-350 g) were used in the present study and were randomly divided into 3 groups (n=8) (control group: CG; BS: Biosilicate and BS/SPG: Biosilicate and SPG). All animals were submitted to the surgical procedure to induce the noncritical size bone defects in tibia of all animals, which were filled with different samples (PINTO et al., 2013). Animals were maintained at the temperature of 22 ± 2ºC, periods of 12 h light–dark, with free access to water and standard food.

Surgical procedure

Before surgery, all animals were submitted to general anesthesia (under sterile conditions), induced by intraperitoneal injection of 20 mg⁄kg xilazin (Anasedan; Sespo Industry and Trade Ltda, Jacareí, SP, Brazil) and 40 mg⁄kg ketamin (Dopalen; Sespo Industry and Trade Ltda, Jacareí, SP, Brazil). Bilateral noncritical, 3 mm diameter, size bone defects were created using motorized drill (Beltec®, Araraquara, SP, Brazil) under copious irrigation with saline solution at the upper third of the tibia, 10 mm distal of the knee joint.

Implants were inserted in the created defect, according to a randomization scheme (n=8 per experimental group). Subsequently, the wounds were closed using a resorbable Vicryl® 5-0 (Johnson&Johnson, St.Stevens-Woluwe, Belgium). Rats were treated with post-surgery cares (i.m., 0.05 mg/kg buprenorphine) (Temgesic; Reckitt Benckiser Health Care Limited, Schering Plough, Hoddesdon, United Kingdom) and were returned to their cages (n=4 per cage). Euthanasia was performed 15 days post-surgery by CO_2 suffocation.

Histopathological analysis

After euthanasia, tibias were retrieved and immediately fixated (in 10% formalin (Merck, Darmstadt, Germany) for 2 days, decalcified in 4% ethylenediaminetetraacetic acid (EDTA) (Merck, Darmstadt, Germany) and dehydrated in a series of ethanol. After that, samples were embedded in paraffin blocks and histological sections were prepared. Sections (5 μm) were prepared trough a microtome (Leica Microsystems SP 1600, Nussloch, Germany) and were stained with hematoxylin and eosin (Merck, Darmstadt, Germany). Laminaes were analyzed using a light microscopy (Leica Microsystems AG, Wetzlar, Germany, Darmstadt-Germany). Qualitative analysis was performed considering the presence of granulation and connective tissue, inflammation, newly formed bone and material particles (PINTO et al., 2013). The analysis was performed by two observers (BD and CG), in a blinded way.

Histomorphometric analysis

Quantitative analysis were performed by the semi-automatic image-analysing OsteoMeasure System (Osteometrics, Atlanta, GA, USA). The following parameters were considered for analysis: osteoblast number per tissue area (N.Ob/T.Ar, $/mm^2$), bone volume fraction (BV/TV, %) and percentage of bone surface occupied by osteoblast (Ob.S/BS). Two experienced observers (BD and CG) performed the analysis, in a blinded way.

Immunohistochemistry analysis

Immunohistochemistry analysis was performed using the streptavidin–biotin-peroxidase method (FANGEL et al., 2014; SANZ-HERRERA and BOCCACCINI, 2011). For this, paraffin was removed with xylene, the specimens were dehydrated in graded ethanol and pre-treated with 0.01 M citric acid buffer (pH 6) in a steamer for 5 min. The endogenous peroxidase was inactivated using the hydrogen peroxide in phosphate-buffered saline (PBS) for 5 min, blocked with 5% normal goat serum in PBS for 10 mins and then incubated with primary antibody (anti-Runx-2 polyclonal (code: sc-8566, Santa Cruz Biotechnology, USA) at a concentration of 1:300), and anti-Rank-L polyclonal (code: sc-7627, Santa Cruz Biotechnology, USA) also at a concentration of 1:300. Biotin-conjugated secondary antibody anti-rabbit IgG (Vector Laboratories, Burlingame, CA, USA) was used for incubation, at a concentration of 1:200 in PBS for 1 h, following by addition of avidin biotin complex conjugated to peroxidase for 45 min. To reveal the immunostaining was used 0.05% solution of 3-3'-diaminobenzidine solution and restrained with Harris haematoxylin (Merck) for 10 second. A qualitative (presence and location of the immunomarkers) and semi-quantitatively assess by using a light microscopy (Leica Microsystems AG, Wetzlar, Germany) were performed. Quantitative analysis according to a previously described scoring scale from 1 to 4 (1 = absent (0% of immunostaining), 2 = weak (1 – 35% of immunostaining), 3 = moderate (36 – 67% of immunostaining), and 4 = intense (68 – 100% of immunostaining) (SWATSCHEK et al., 2002; SHIN et al., 2003). The analysis was performed in a blinded way (CG and GCAV).

Biomechanical test

Three-point bending test was performed using a Instron® Universal Testing Machine (Instron® Worldwide Headquarters, Norwood, MA, USA, 3342 model and 500 N load cell). For testing, samples were placed on a device (3.8 cm) (1.8 cm distant double support on the diaphysis). The load cell was perpendicularly positioned at the middle point of the tibiae and the bending force was used at a constant deformation rate (0.5 cm/min) until the fracture occurred. Finally, the maximum load (N), resilience (J) and force of fracture (N) were measured from the load-deformation obtained (UENO et al., 2016; ZHANG et al., 2018).

Statistical analysis

Data were analysed and displayed in graphs, and the values expressed as mean and standard deviation. In the statistical analysis, the distribution of variables was tested using the Shapiro-Wilk normality test. For the analysis of multiple comparisons, ANOVA was used with post hoc Tukey for parametric data and nonparametric

data, the Kruskal-Wallis test was used with post hoc Dunn. The level of significance was set at 5 % ($p \leq 0.05$). All statistical analyses were performed using GraphPad Prism version 6.01.

RESULTS

SEM

SEM representative micrographs of BS and BS/SPG are depicted in Fig. 1. PMMA microspheres and the bio ceramic material can be observed in both samples. Furthermore, BS presented a more homogeneous surface topography with the presence of few pores. For BS/SPG, PMMA microspheres and biosilicate particles surrounded by sponging was observed. Additionally, it is possible to see the presence of plenty pores and an irregular surface topography.
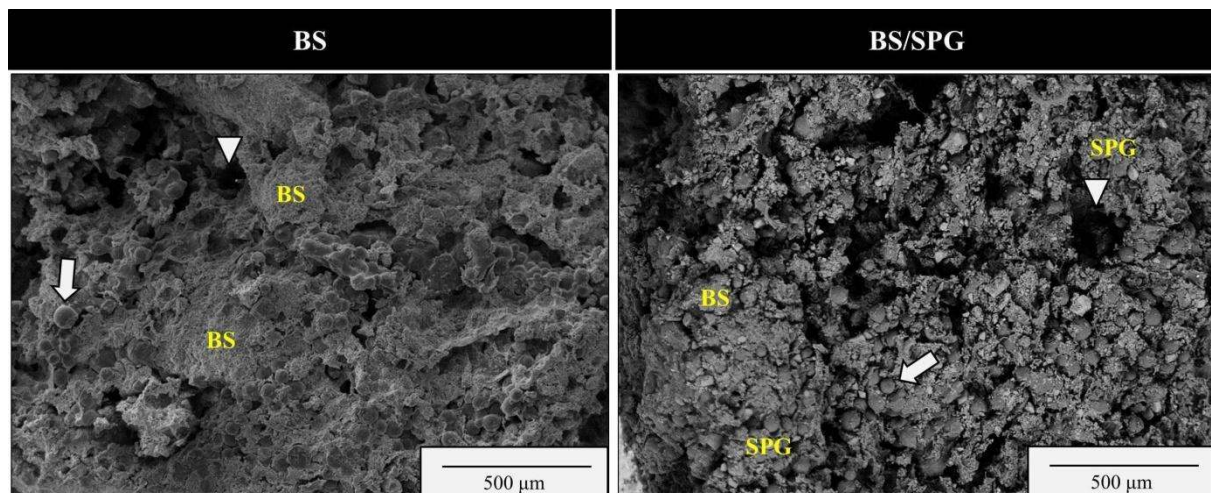

Figure 1. SEM representative micrographs of cross-sections BS and BS/SPG. Pores (white arrows head); PMMA (white arrows); Biosilicate (BS) and Spongin (SPG) are indicated in the SEM micrographs. Bar represents 500 μm.

Histopathological analysis

Figure 2 demonstrates representative histological sections for CG, BS and BS/SPG 15 days post-surgery. An overview of the defect area can be observed for all the experimental groups, at 2 different magnitudes (20 and 40xmag). For CG, most of the defect was filled by newly formed bone and some areas filled of granulation tissue especially in the center of the defect. For BS, it is possible to verify the presence of areas of newly formed bone, mainly at the borders, and granulation tissue. The center of defect was occupied by a residual material and granulation tissue. In the BS/SPG, it is possible to observe some degradation of material, but its presence was notable, mainly in the center of the defect. Granulation tissue was filling most of the defect area with some newly formed bone at the borders.
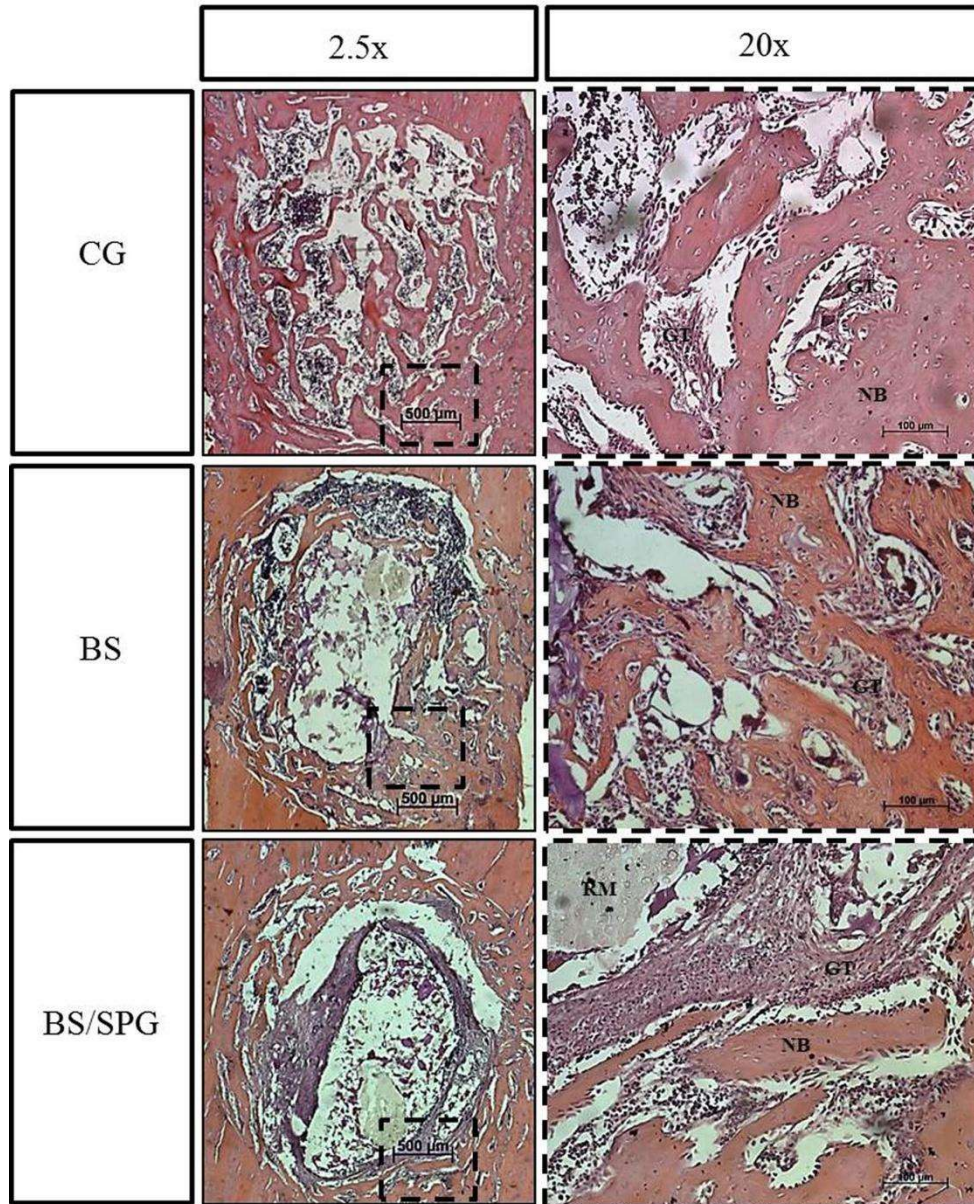
Figure 2. Representative histological sections of CG, BS and BS/SPG groups after 15 days. GT: granulation tissue; NB: newly bone; RM: residual material. Hematoxylin and eosin. Scale bar: 500 µm (mag. x2.5); 100 µm (mag. x20).

Histomorphometric analysis

Figure 3 demonstrated the values for the histomorphometry analysis. CG demonstrated a higher value of % BV/TV compared to BS and BS/SPG (*$p<0.05$ and **$p<0.01$, respectively) (Fig. 3A). Moreover, for BS/SPG, a lower value was observed compared to BS.
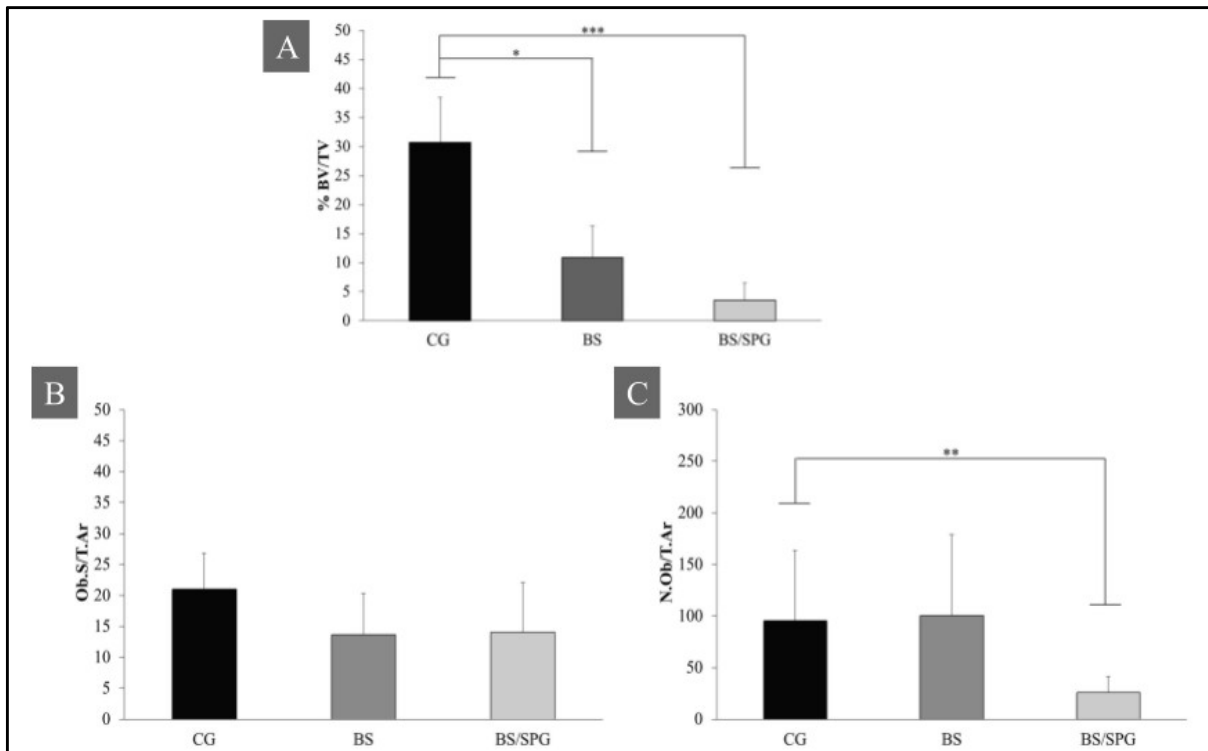
Figure 3. Means and standard deviation of bone volume as a percentage of tissue volume BV/TV % (A), osteoblast surface per tissue area Ob.S/T.Ar % (B) and number of osteoblasts per tissue area N.Ob/T.Ar, mm2 (C). Dunn`s test.

Additionally, for Ob.S/T.Ar, no difference was found among the groups (Fig. 3B) and for N.Ob/T.Ar, a lower value was observed in BS/SPG (Fig. 3C).

Immunohistochemistry

Qualitative analysis of Runx-2

Positive Runx-2 immunostaining was observed in all experimental groups 15 days post-surgery (Fig. 4). For CG, Runx-2 immunostaining was observed mainly in granulation tissue and in the newly formed bone. Furthermore, both biomaterial groups (BS and BS/SPG) demonstrated a Runx-2 immunostaining predominantly in the granulation tissue and in the newly formed bone. Additionally, the presence of Runx-2 was detected between the biomaterial particles for both BS and BS/SPG (Fig. 4).
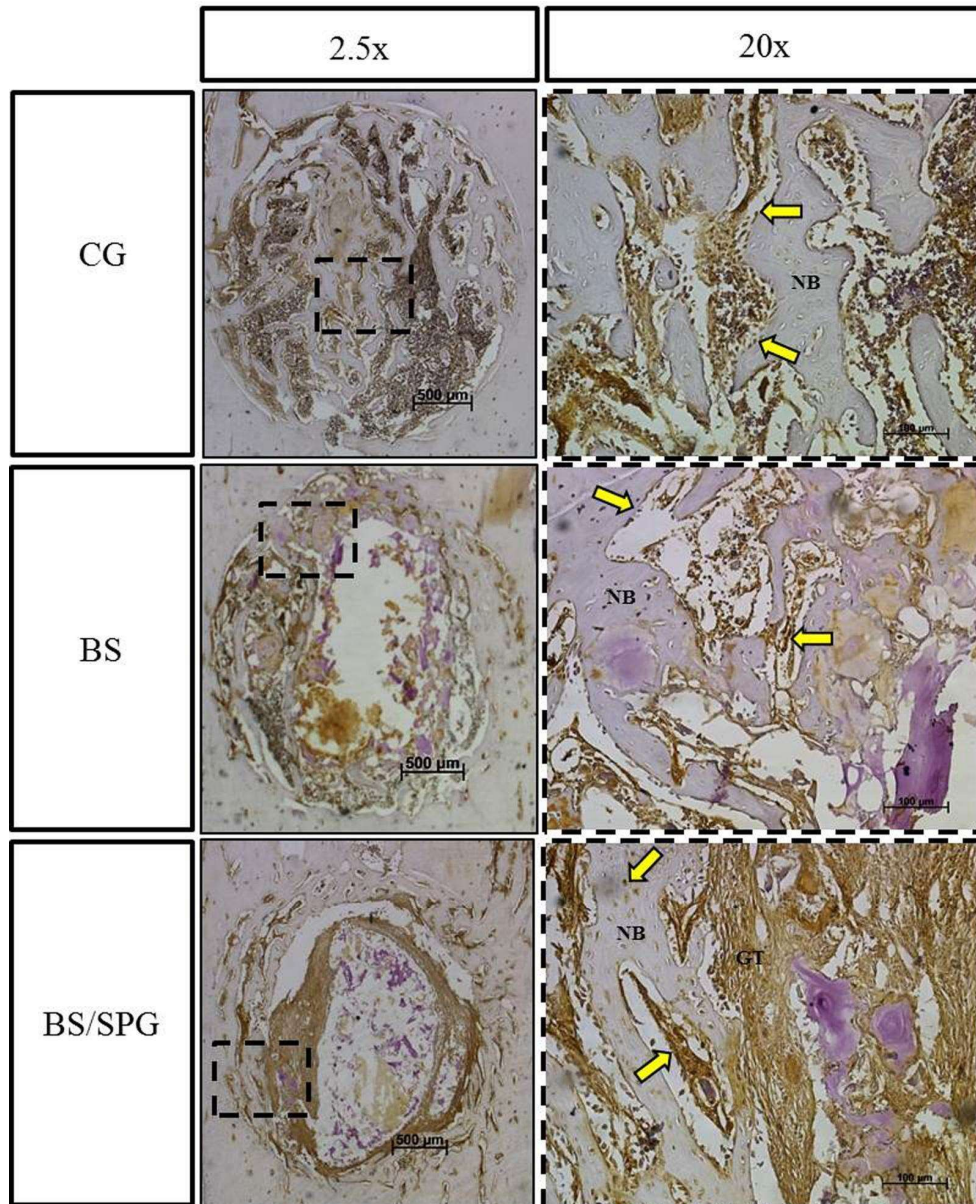
Figure 4. Immunohistochemistry of Runx-2 for CG, BS and BS/SPG groups after 15 days post-surgery. NB: newly formed bone; GT: granulation tissue and arrows indicates Runx-2 immunostaining. Scale bar: 500 μm (mag. x2.5) and 100 μm (mag. x20).

Semi-quantitative analysis of Runx-2

Figure 5 presented the semi-quantitative analysis of Runx-2 immunostaining. No significant difference in Runx-2 immunostaining was found among the groups.
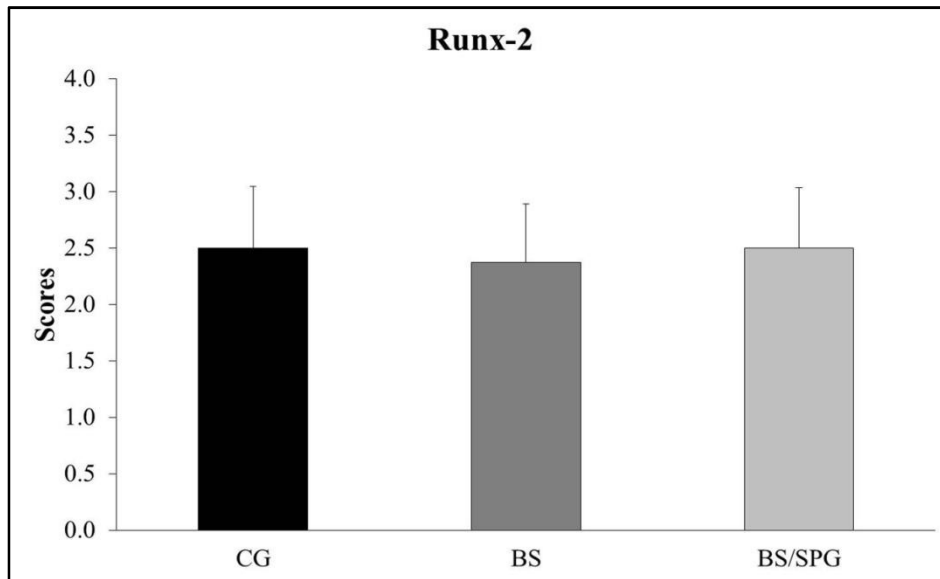
Figure 5. Means and standard deviation of scores immunohistochemistry of Runx-2 for CG, BS and BS/SPG groups after 15 days post-surgery. Dunn`s test.

Qualitative analysis of Rank-L

Rank-L immunolabeling was observed in all experimental groups (Fig. 6). For CG group, the predominance of Rank-L immunostaining was observed in granulation tissue. Moreover, for BS and BS/SPG groups, the immunostaining was more evidenced in granulation tissue and newly formed bone. Interestingly, Rank-L immunostaining could be observed in the BS and BS/SPG groups between the particles of the material, especially in the center of the defect.
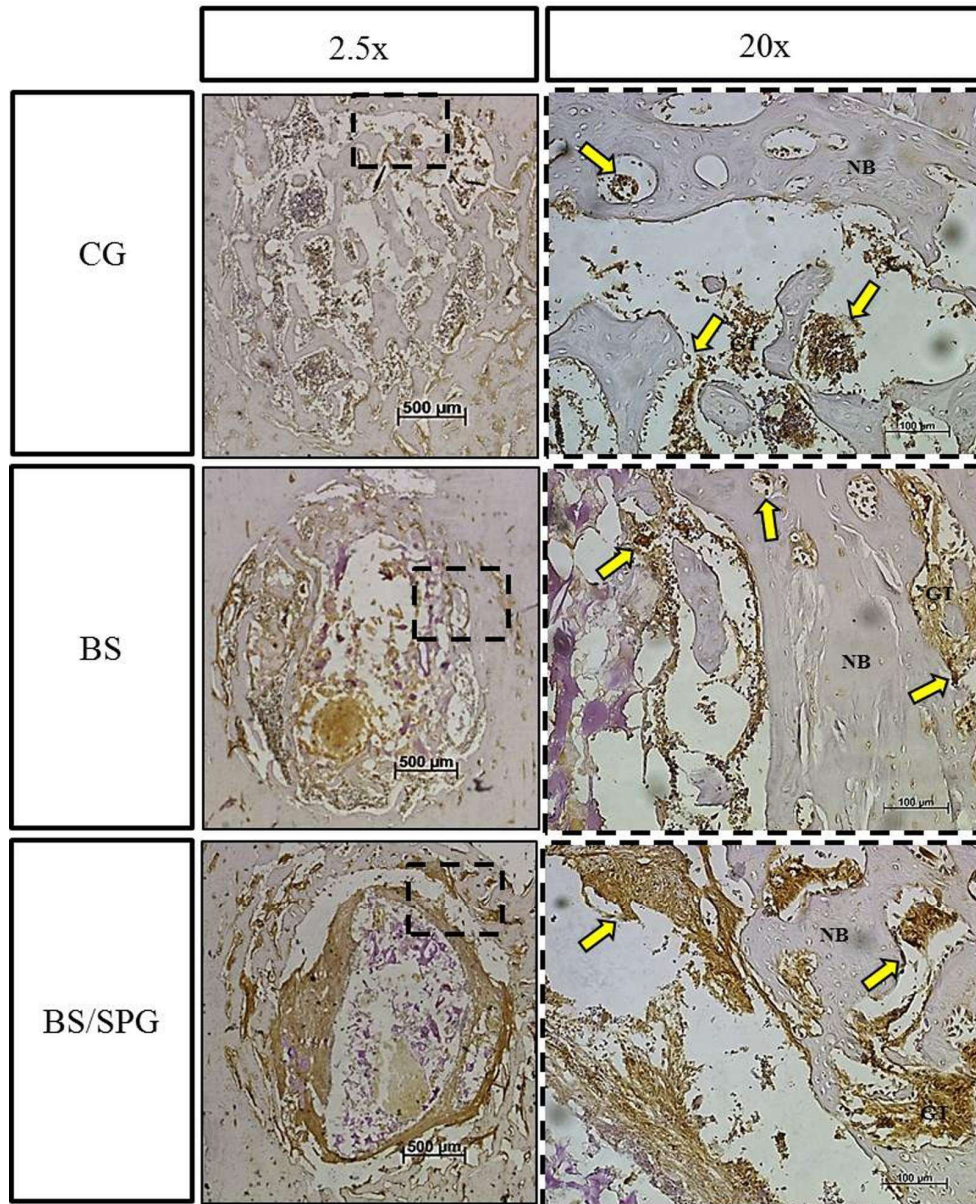
Figure 6 Immunohistochemistry of Rank-L for CG, BS and BS/SPG groups after 15 days post-surgery. NB: newly formed bone; GT: granulation tissue and arrows indicates Rank-L immunostaining. Scale bar: 500 µm (mag. x2.5) and 100 µm (mag. x20)

Semi-quantitative analysis of Rank-L

Figure 7 shows immunostaining of Rank-L in CG, BS and BS/SPG after 15 days post-surgery. No significant difference was observed among the groups for Rank-L immunolabeling.
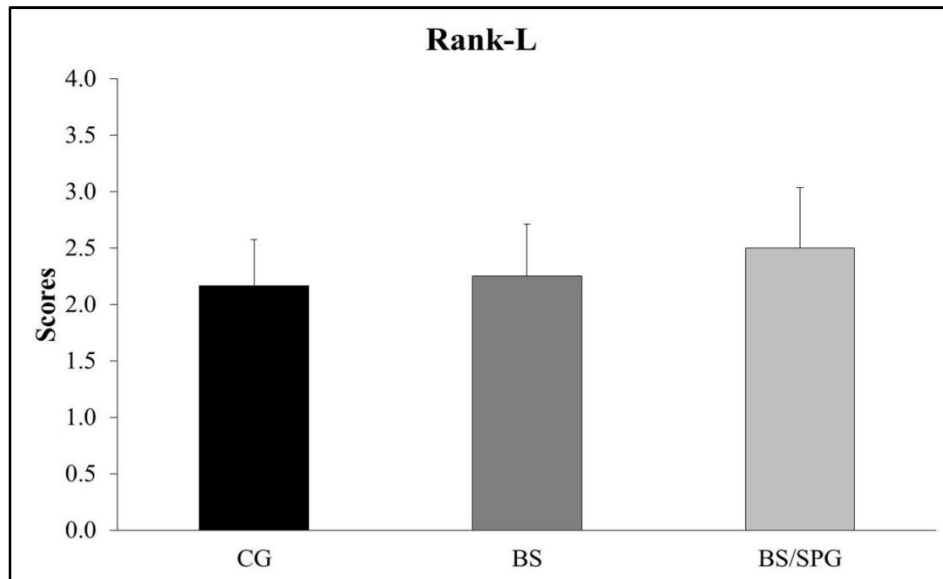
Figure 7. Means and standard deviation of scores immunohistochemistry of Rank-L for CG, BS and BS/SPG groups after 15 days post-surgery. Dunn`s test.

Biomechanical test

For the biomechanical test, no significant differences were observed in Maximum Load, Force of Fracture and Resilience analysis for any experimental group studied in this work (Fig. 8).
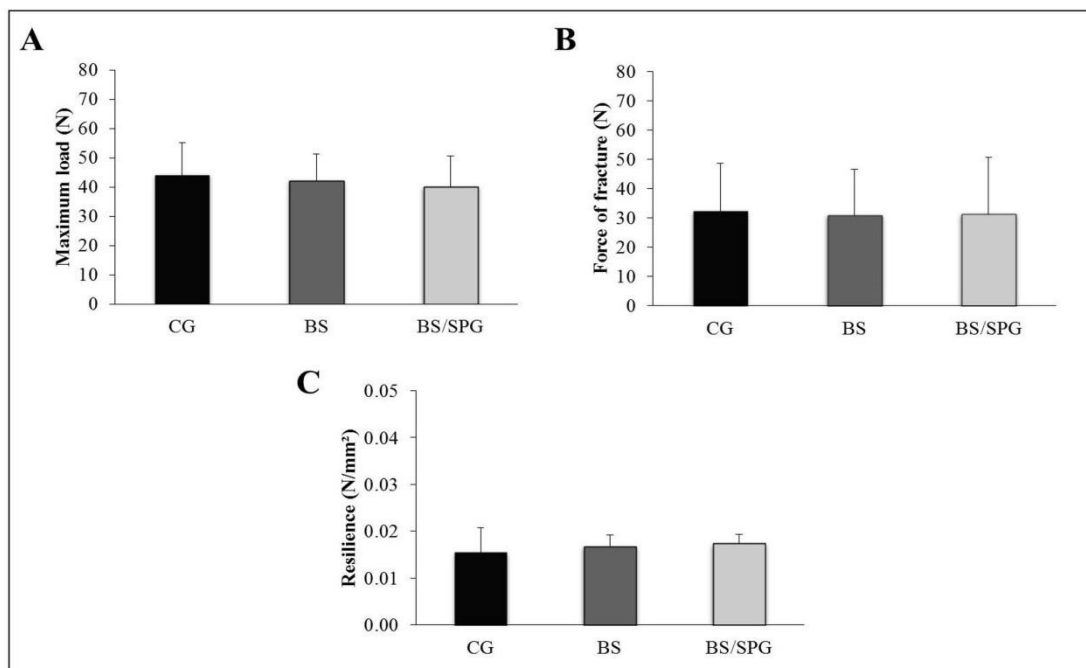

Figure 8. Means and standard deviation of **A:** Maximum load (N); **B:** Force of fracture (N) and **C:** Resilience (N/mm^2) for CG, BS and BS/SPG groups after 15 days post-surgery. Dunn`s test.

DISCUSSION

The present study investigated the incorporation of an organic component (marine SPG) into a BS, aiming to produce a biomimetic bone composite using an in vivo experimental model of tibial bone defect in rats. The histological analysis demonstrated that for BS, newly formed bone ingrowth was observed into the defect area and for BS/SPG composite treated animals, bone defects were filled mostly by granulation tissue. Moreover, histomorphometry analysis demonstrated lower values of %BV/TV and N.Ob/T.Ar for BS/SPG. Interestingly, no difference of Runx-2 and Rank-L immunostaining was observed between the experimental groups. Additionally, biomechanical analysis demonstrated similar values for all the groups.

SPG incorporation into BS and composite manufacturing were successfully obtained by the methods used, demonstrating adequate mechanical properties and easy to handle. It is worthwhile to mention that the formulation of the composites were bioinspired and aimed to mimic bone composition (LONG et al., 2015). SEM micrographs demonstrated that SPG were well distributed into BS and pores were presented into the composites.

As mentioned before, BS has successfully been used for bone tissue engineering proposes and its osteogenic effects and ability to stimulate bone tissue have been demonstrated by many authors (AFZAL et al., 2004; GABBAI-ARMELIN et al., 2017; KOMORI, 2011). It is well known that, the ions released from the biomaterial after implantation into tissues beneficially affects osteogenesis by forming a silica layer, which guides new bone formation (MOURA et al., 2007). Moreover, the rate of BS degradation seems to be appropriate, which culminate in more space for tissue ingrowth. In the present study, the higher amount of newly formed bone tissue observed in the BS treated animals can be explained by the high bioactivity rate of the glass ceramic associated to the degradation of the material (KEARNS et al., 2008).

Interestingly, the association of BS and SPG has not stimulates a higher deposition of bone tissue. Col is important to attract bone cells and support their growth and proliferation and it has been widely used for bone tissue engineering (WADA et al., 2006). However, as an explanation of the lack of optimized results in the process of healing of the composite treated animals, it is possible to state that the addition of marine collagen into BS may have overstimulated bone metabolism, which may have avoided tissue to further respond to the composite. These findings corroborate those of Parisi et al. (2020) who found that a composite made of BS (80%), SPG (20%) and Poly (methyl methacrylate) (used to aggregate the material) did not produce any improvement in the bone healing in a critical model of cranial bone defect in rats after after two and six weeks of implantation. Conversely, Long et al. (2015) demonstrated that BG/Collagen scaffolds presented adequate biocompatibility, mechanical stability and porosity, allowing proliferation of human bone marrow stromal cells.

Although the presence of Runx-2 immunostainning for all groups, no statistical difference was observed. Runx-2 stimulates the differentiation of mesenchymal progenitors toward osteoblast cell lineage (HOERTH et al., 2014; TOLEDANO et al., 2018). In addition, it is known that Runx-2 is a transcription factor expressed mainly in the initial repair periods and influences the activation of several osteogenic markers such as osteopontin, alkaline phosphatase and RANK-L (OSTERHOFF et al., 2016; QASIM et al., 2019; WADA et al., 2006). At this moment, it is still unclear the reasons for the lack of difference, but possibly the materials used did not offer any extra stimulus to increase the labelling of this immunomarker in the experimental period evaluated. Similarly, RANK-L immunostaining was detected for all groups but also, with no statistical difference. It is well known that RANK-L is a key factor for differentiation and activation of osteoclasts and that Runx2 is responsible by regulating RANK-L and consequently osteoclastogenesis (OSORIO et al., 2020; TOLEDANO et al., 2018; WANG et al., 2017). It can be hypothesized the lack of difference in the expression of Runx-2 resulted in no difference of RANK-L imunnostaining.

Similar results among groups were observed in the biomechanical tests. Bone mechanical behavior depends not only on its geometry and architecture but also on its tissue composition (CHEN and LIU, 2016; FERNANDEZ et al., 2018). Bone mass, as well as the quality and arrangement of its microstructural elements, influences bone mechanical properties (DROSSE et al., 2008; DIAZ-RODRIGUEZ et al., 2018; FERNANDEZ et al., 2018). Therefore, the similar bone biomechanical properties observed for all groups can be seen as a positive aspect and probably indicate that the presence of the materials and/or spatial distribution associated to the granulation tissue or newly formed bone culminated in the same bone strength.

It is necessary to emphasize that the bone defect model used in the present study was a non-critical one, which means that the process of healing happen spontaneously (FERNANDES et al., 2019). In this context, in order to progress the understanding of the effects of the composite scaffold in the process of healing, the use of a critical model is necessary to evaluate in more details the behavior of the materials in the process of non-spontaneous healing. As the present study was limited to relatively short-term evaluation of the performance of present biomaterials used, detailed information on the long-term performance of BS/SPG composites needs to be provided. Following this line, further investigations are necessary to validate these combinations as safe and efficient materials for biomedical applications.

CONCLUSIONS

BS showed promising results in the stimulation of bone healing and newly formed bone deposition. Interestingly, BS/SPG treated animals, in the composition used (70/30) presented mainly granulation tissue filling the defect area. Furthermore, similar results were found for Runx-2 and RANK-L immunostaining and biomechanical analysis. Further researches are required to evaluate the biological performance of BS/SPG in compromised situations (such as non-critical models), different material formulations and long-term studies

REFERENCES

AFZAL, F.; POLAK, J.; BUTTERY, L. Endothelial nitric oxide synthase in the control of osteoblastic mineralizing activity and bone integrity. **Journal of Pathology,** v.202, p.503-510, 2004.

AMINI, A.R.; LAURENCIN, C.T.; NUKAVARAPU, S.P. Bone tissue engineering: recent advances and challenges. **Critical Reviews in Biomedical Engineering,** v.40, p.363-408, 2012.

BOSSINI, P.S.; RENNÓ, A.C.M.; RIBEIRO, D.A.; FANGEL, R.; PEITL, O.; et al. Biosilicate® and low-level laser therapy improve bone repair in osteoporotic rats. **Journal of Tissue Engineering and Regenerative Medicine,** v.12, p.52-57, 2011.

CAPUZZO, E.; STEPHENS, D.; SILVA, T.; BARRY, J.; FORSTER, R.M. Decrease in water clarity of the southern and central North Sea during the 20th century. **Global Change Biology,** v.21, p.2206-2214, 2015.

CHEN, F.M.; LIU, X. Advancing biomaterials of human origin for tissue engineering. **Progress in Polymer Science,** v.1, p.86-168, 2016.

COLE, J.H.; VAN DER MEULEN, M.C. Whole bone mechanics and bone quality. **Clinical Orthopaedics and Related Research,** v.469, p.2139-2149, 2011.

DIAZ-RODRIGUEZ, P.; SÁNCHEZ, M.; LANDIN, M. Drug-Loaded Biomimetic Ceramics for Tissue Engineering. **Pharmaceutics.,** v.10, p.272, 2018.

DROSSE, I.; VOLKMER, E.; CAPANNA, R.; DE BIASE, P.; MUTSCHLER, W.; SCHIEKER, M. Tissue engineering for bone defect healing: an update on a multi-component approach. **Injury,** v.39, p.S9-S20, 2008.

EINHORN, T.A. New technologies for the enhancement of skeletal repair: Challenges and opportunities. **Indian Journal of Orthopaedics,** v.45, p.489-491, 2011.

EXPOSITO, J.Y.; CLUZEL, C.; GARRONE, R.; LETHIAS, C. Evolution of collagens. **The Anatomical Record,** v.268, p.302-316, 2002.

EZIRGANLI, S.; KAZANCIOGLU, H.O.; MIHMANLI, A.; SHARIFOV, R.; AYDIN, M.S. Effects of different biomaterials on augmented bone volume resorptions. **Clinical Oral Implants Research,** v.26, p.1482-1488, 2015.

FANGEL, R.; BOSSINI, P.S.; RENNO, A.C.; GRANITO, R.N.; WANG, C.C.; NONAKA, K.O.; et al. Biomechanical properties: effects of low-level laser therapy and Biosilicate® on tibial bone defects in osteopenic rats**. Journal Applied Biomaterials & Functional Materials,** v.12, p.271-7, 2014.

FERNANDES, K.R.; MAGRI, A.M.P.; KIDO, H.W.; PARISI, J.R.; ASSIS, L.; FERNANDES, K.P.S.; et al. Biosilicate/PLGA osteogenic effects modulated by laser therapy: In vitro and in vivo studies. **Journal of Photochemistry and Photobiology B: Biology,** v.173, p.258-265, 2017.

FERNANDES, K.R.; PARISI, J.R.; MAGRI, A.M.P.; KIDO, H.W.; GABBAI-ARMELIN, P.R.; FORTULAN, C.A.; et al. Influence of the incorporation of marine spongin into a Biosilicate®: an in vitro study. **Journal of Materials Science: Materials in Medicine,** v.30, p.64, 2019.

FERNANDEZ DE GRADO, G.; KELLER, L.; IDOUX-GILLET, Y.; WAGNER, Q.; MUSSET, A.M.; BENKIRANE-JESSEL, N.; BORNERT, F.; OFFNER D. Bone substitutes: a review of their characteristics, clinical

use, and perspectives for large bone defects management. **Journal of Tissue Engineering,** v. 9, p.2041731418776819, 2018.

GABBAI-ARMELIN, P.R.; SOUZA, M.T.; KIDO, K.H.; TIM, C.R.; BOSSINI, P.S.; FERNANDES, K.R.; et al. Characterization and biocompatibility of a fibrous glassy scaffold. **Journal of Tissue Engineering and Regenerative Medicine,** v.11, p.1141-1151, 2017.

GRANITO, R.N.; RENNO, A.C.; RAVAGNANI, C.; BOSSINI, P.S.; MOCHIUTI, D.; JORGETTI, V.; et al. In vivo biological performance of a novel highly bioactive glass-ceramic (Biosilicate®): A biomechanical and histomorphometric study in rat tibial defects. **Journal of Biomedical Materials Research Part B Applied Biomaterials**, v. 97, p.139-47, 2011.

GRANITO, R.N.; RIBEIRO, D.A; RENNÓ, A.C.M; RAVAGNANI, C.; BOSSINI, P.S.; PEITLFILHO, O.; ZANOTTO, E.D.; PARIZOTTO, N.A. Effects of biosilicate and bioglass 45S5 on tibial bone consolidation on rats: a biomechanical and a histological study. **Journal of Materials Science: Materials in Medicine,** v. 20, p. 2521-2526, 2009.

GREEN, D; HOWARD, D; YANG, X; KELLY, M; OREFFO, R.O.C. Natural Marine Sponge Fiber Skeleton: A Biomimetic Scaffold for Human Osteoprogenitor Cell Attachment, Growth, and Differentiation. **Tissue Engineering,** 9(6):1159-66, 2003.

HÄGG, P.; VÄISÄNEN, T.; TUOMISTO, A.; REHN, M.; TU, H.; HUHTALA, P.; ESKELINEN, S.; PIHLAJANIEMI, T. Type XIII collagen: a novel cell adhesion component present in a range of cell-matrix adhesions and in the intercalated discs between cardiac muscle cells. **Matrix Biology,** v.19, p.727-42, 2001.

HENCH, L.L.; JONES, J.R. Bioactive Glasses: Frontiers and Challenges. **Front Bioeng Biotechnol.,** v.3, p.1–12, 2015.

HOERTH, R.M.; SEIDT, B.M.; SHAH, M.; SCHWARZ, C.; WILLIE, B.M.; DUDA, G.N.; et al. Mechanical and structural properties of bone in non-critical and critical healing in rat. In: **Acta Biomaterialia,** v.10, p.4009-4019, 2014.

HUANG, Y.Y.; SHARMA, S.K.; CARROLL, J.; HAMBLIN, M.R. Biphasic dose response in low level light therapy - an update. **Dose-response: a publication of International Hormesis Society,** v. 9, p.602–618, 2011.

IWATSUBO, T.; KISHI, R.; MIURA, T.; OHZONO, T.; YAMAGUCHI, T. Formation of Hydroxyapatite Skeletal Materials from Hydrogel Matrices via Artificial Biomineralization. **Journal of Physical Chemistry B.,** v.119, p.8793-8799, 2015.

KEARNS, A.E.; KHOSLA, S.; KOSTENUIK, P.J. Receptor activator of nuclear factor kappaB ligand and osteoprotegerin regulation of bone remodeling in health and disease. **Endocrine Reviews,** v.29, p.155-192, 2008.

KIDO, H.W.; BRASSOLATTI, P.; TIM, C.R.; GABBAI-ARMELI, P.R.; MAGRI, A.M.P.; FERNANDES, K.R.; et al. Porous poly (D,L-lactide-co-glycolide) acid/biosilicate® composite scaffolds for bone tissue engineering. **Journal of Biomedical Materials Research Part B Applied Biomaterials,** v.105, p.63-71, 2015.

KIDO, H.W; GABBAI-ARMELIN, P.R; AVANZI, I.R; SILVA, A.C; FERNANDES, K.R; FORTULAN, C.A; RENNÓ, A.C.M. Vacuumed collagen-impregnated bioglass scaffolds: Characterization and influence on proliferation and differentiation of bone marrow stromal cells. **Journal of Biomedical Materials Research Part B Applied Biomaterials,** 107(2):211-222, 2019.

KIDO, H.W.; RIBEIRO, D.A.; DE OLIVEIRA, P.; PARIZOTTO, N.A.; CAMILO, C.C.; FORTULAN, C.A.; MARCANTONIO, E.J.R.; DA SILVA, V.H.; RENNO, A.C. Biocompatibility of a porous alumina ceramic scaffold coated with hydroxyapatite and bioglass. **Journal of biomedical materials research. Part A,** v.102, p.2072–2078, 2014.

KOMORI, T. Signaling networks in RUNX2-dependent bone development. **Journal of Cellular Biochemistry,** v.112, p.750-5, 2011.

KUTTAPPAN, S.; MATHEW, D.; NAIR, M.B. Biomimetic composite scaffolds containing bioceramics and collagen/gelatin for bone tissue engineering - A mini review. **International Journal of Biological Macromolecules,** v.93, p.1390–401, 2016.

LIAO, S.S.; CUI, F.Z.; ZHANG, W.; FENG, Q.L. (2004). Hierarchically biomimetic bone scaffold materials: nano-HA/collagen/PLA composite. **Journal of Biomedical Materials Research Part B Applied Biomaterials,** v.69, p.158–165, 2004.

LIN, Z.; SOLOMON, K.L.; ZHANG, X.; PAVLOS, N.J.; ABEL, T.; WILLERS, C.; DAI, K.; XU, J.; ZHENG, Q.; ZHENG, M. In vitro evaluation of natural marine sponge collagen as a scaffold for bone tissue engineering. **International Journal of Biological Sciences,** v.7, p.968-77, 2011.

LIRANI-GALVÃO, A.P.; JORGETTI, V.; DA SILVA, O.L. Comparative study of how low-level laser therapy and low-intensity pulsed ultrasound affect bone repair in rats. **Photomedicine and Laser Surgery,** v.24, p.735-40, 2006.

LONG, T.; YANG, J.; SHI, S.S.; GUO, Y.P.; KE, Q.F.; ZHU, Z.A. Fabrication of three-dimensional porous scaffold based on collagen fiber and bioglass for bone tissue engineering. **Journal of Biomedical Materials Research Part B Applied Biomaterials,** v.103, p.1455-64, 2015.

LOPEZ-HEREDIA, MA.; SAA, Y.; SALMONC, P.; DE WIJNA, J.R.; WOLKEA, J.G.C.; JANSEN, J.A. Bulk properties and bioactivity assessment of porous polymethylmethacrylate cement loaded with calcium phosphates under simulated physiological conditions. **Acta Biomaterialia,** v.8, p.3120-3127, 2012.

MAGRI, A.M.; FERNANDES, K.R.; ASSIS, L.; MENDES, N.A.; SANTOS, A.L.Y.S.; DANTAS, E.O.; RENNO A.C. Photobiomodulation and bone healing in diabetic rats: evaluation of bone response using a tibial defect experimental model. **Lasers in Medical Science,** v.30, p.1949-57, 2015.

MATSUMOTO, MA; CAVIQUIOLI, G; BIGUETTI, CC; HOLGADO, LA; SARAIVA, PP; RENNÓ, ACM; KAWAKAMI, RY. A novel bioactive vitroceramic presents similar biological responses as autogenous bone grafts. **Journal of Materials Science: Materials in Medicine,** v.23, p.1447-56, 2012.

MOURA, J.; TEIXEIRA, L.N.; RAVAGNANI, C.; PEITL, O.; ZANOTTO, E.D.; BELOTI, M.M.; PANZERI, H.; ROSA, A.L.; DE OLIVEIRA, P.T. In vitro osteogenesis on a highly bioactive glass-ceramic (Biosilicate). **Journal of Biomedical Materials Research Part A,** v.82, p.545-57, 2007.

OLIVEIRA, F.S.; PINFILDI, C.E.; PARIZOTO, N.A.; LIEBANO, R.E.; BOSSINI, P.S.; GARCIA, E.B.; FERREIRA, L.M. Effect of low level laser therapy (830 nm) with different therapy regimes on the process of tissue repair in partial lesion calcaneous tendon. **Lasers in Surgery and Medicine,** v.41, p.271-6, 2009.

OSORIO, C.C.; ESCOBAR, L.M.; GONZÁLEZ, M.C.; GAMBOA, L.F.; CHAMBRONE, L. Evaluation of density, volume, height and rate of bone resorption of substitutes of autologous bone grafts for the repair of alveolar clefts in humans: A systematic review. **Heliyon.**, v.6, p.e04646, 2020.

OSTERHOFF, G.; MORGAN, E.F.; SHEFELBINE, S.J.; KARIM, L.; MCNAMARA, L.M.; AUGAT P. Bone mechanical properties and changes with osteoporosis. **Injury,** v.47, p.S11-20, 2016.

PARISI, J.R.; FERNANDES, K.R.; APARECIDA DO VALE, G.C.; SANTANA, A.F.; CRUZ, M.A.; FORTULAN, C.A.; ZANOTTO, E.D.; et al. Marine spongin incorporation into Biosilicate® for tissue engineering applications: An in vivo study. **Journal of Biomaterials Applications,** v.35, p.205-214, 2020.

PARISI, J.R.; FERNANDES, K.R.; AVANZI, I..; DORILEO, B.P.; SANTANA, A.F.; ANDRADE, A.L.; GABBAI-ARMELIN, P.R.; FORTULAN, C.A.; TRICHÊS, E.S.; GRANITO, R.N.; RENNO, A.C.M. Incorporation of Collagen from Marine Sponges (Spongin) into Hydroxyapatite Samples: Characterization and In Vitro Biological Evaluation. **Marine Biotechnology,** v.21, p. 30–37, 2019.

PETTIAN, M.S.; PLEPIS, A.M.G.; MARTINS, V.D.C.A.; DOS SANTOS, G.R.; PINTO, C.A.L.; GALDEANO, E.A.; CALEGARI, A.R.A.; DE MORAES, C.A.; CUNHA, M.R.D. Use of an anionic collagen matrix made from bovine intestinal serosa for in vivo repair of cranial defects. **PLoS One,** v.13, 2018.

PINTO, K.N.; TIM, C.R.; CROVACE, M.C.; MATSUMOTO, M.A.; PARIZOTTO, N.A.; ZANOTTO, E.D.; PEITL, O.; RENNO, A.C. Effects of Biosilicate® scaffolds and low-level laser therapy on the process of bone healing. **Photomedicine and Laser Surgery,** v.31, p.252-60, 2013.

QASIM, M.; CHAE, D.S.; LEE, N. Y. Advancements and frontiers in nano-based 3D and 4D scaffolds for bone and cartilage tissue engineering. **Internation Journal of Nanomedicine,** v.14, p.4333–4351, 2019.

REZWAN, K.; CHEN, Q.Z.; BLAKER, J.J.; BOCCACCINI, A.R. Biodegradable and bioactive porous polymer/inorganic composite scaffolds for bone tissue engineering. **Biomaterials,** v.27, p.3413-3431, 2006.

RIZWAN, M.; HAMDI, M.; BASIRUN, W.J. Bioglass® 45S5-based composites for bone tissue engineering and functional applications. **Journal of Biomedical Materials Research Part A,** v.105, p.3197-3223, 2017.

SANZ-HERRERA, J.A.; BOCCACCINI, A.R. Modelling bioactivity and degradation of bioactive glass based tissue engineering scaffolds. **International Journal of Solids and Structures,** v.48, p.257-268. 2011.

SHIN, H.; QUINTEN RUHÉ, P.; MIKOS, A.G.; JANSEN, J.A. In vivo bone and soft tissue response to injectable, biodegradable oligo(poly(ethylene glycol) fumarate) hydrogels. **Biomaterials,** v.24, p.3201–3211, 2003.

SILVA, T.H.; MOREIRA-SILVA, J.; MARQUES, A.L.; DOMINGUES, A.; BAYON, Y.; REIS, R.L. Marine origin collagens and its potential applications. **Marine drugs,** v.12, p.881-5901, 2014.

SWATSCHEK, D.; SCHATTON, W.; KELLERMANN, J.; MÜLLER, W.E.; KREUTER, J. Marine sponge collagen: isolation, characterization and effects on the skin parameters surface-pH, moisture and sebum. **European Journal of Pharmaceutics and Biopharmaceutics,** v.53, p.107-113, 2002.

TOLEDANO, M.; TOLEDANO-OSORIO, M.; GUERADO, E.; CASO, E.; OSORIO, E.; OSORIO, R. Assessing bone quality through mechanical properties in postmenopausal trabecular bone. **Injury,** v.49, p.S3-S10, 2018.

UENO, F.R.; KIDO, H.W.; GRANITO, R.N.; GABBAI-ARMELIN, P.R.; MAGRI, A.M.; FERNANDES, K.R.; et al. Calcium phosphate fibers coated with collagen: In vivo evaluation of the effects on bone repair. **Bio-Medical Materials and Engineering,** V.27, p.259–27, 2016.

WADA, T.; NAKASHIMA, T.; HIROSHI, N.; PENNINGER, J.M. RANKL-RANK signaling in osteoclastogenesis and bone disease. **Trends in Molecular Medicine,** v.12, p.17-25, 2006.

WANG, L.; YOON, D.M.; SPICER, P.P.; HENSLEE, A.M.; SCOTT, D.W.; WONG, M.E.; et al. Characterization of porous polymethylmethacrylate space maintainers for craniofacial reconstruction. **Journal of Biomedical Materials Research Part B Applied Biomaterials**, v.101, p.813-825, 2013.

WANG, W.; YEUNG, K.W.Y. Bone grafts and biomaterials substitutes for bone defect repair: A review. **Bioactive Materials,** v.2, p.224-247, 2017.

WILLIAMS, D.F. To engineer is to create: The link between engineering and regeneration. **Trends in Biotechnology,** v.24, p.4-8, 2006.

ZHANG, D.; WU, X.; CHEN, J.; LIN, K. The development of collagen based composite scaffolds for bone regeneration. **Bioactive Materials,** v.3, p.129-138, 2018.

ZHAO, S.; WANG, H.; ZHANG, Y.; HUANG, W.; RAHAMAN, M.N.; LIU, Z.; WANG, D.; ZHANG, C. Copper-doped borosilicate bioactive glass scaffolds with improved angiogenic and osteogenic capacity for repairing osseous defects. **Acta biomaterialia,** v.14, p.185–196, 2015.